Inorganic Chemistry

Article

pubs.acs.org/IC

Predesign and Systematic Synthesis of 11 Highly Porous Coordination Polymers with Unprecedented Topology

Jingui Duan,*[,†,‡] Masakazu Higuchi,[†] and Susumu Kitagawa*[,†]

[†]Institute for Integrated Cell-Material Sciences (WPI-iCeMS), Kyoto University, Yoshida, Sakyo-ku, Kyoto, 606-8501, Japan

[‡]State Key Laboratory of Materials-Oriented Chemical Engineering, College of Chemistry and Chemical Engineering, Nanjing Tech University, Nanjing 210009, China

Supporting Information

ABSTRACT: We propose and validate a simple strategy of vertex connection that can be used for framework design and pore size/type modulation to prepare a mother structure and another 10 highly porous isoreticular frameworks with unprecedented topology. Importantly, the potential accessible pore volumes (57−71%), pore sizes (6.8−11. 2 Å; 17.0−29.0 Å; 12.5−22.8 Å; 11.9−24.5 Å), and the pore shapes of this series of highly porous frameworks were simultaneously and systematically tuned. Interestingly, the pore size of IIa $[Zn_4O(L^2)_2(BDC)_{0.5}]$-$\{(CH_3)_2NH_2\}$ decreased a little less than that of IIc $[Zn_4O(L^2)_2(2,6\text{-}NDC)_{0.5}]\{(CH_3)_2NH_2\}$; however, its selectivity of CO_2 toward CH_4 increased by almost two times.

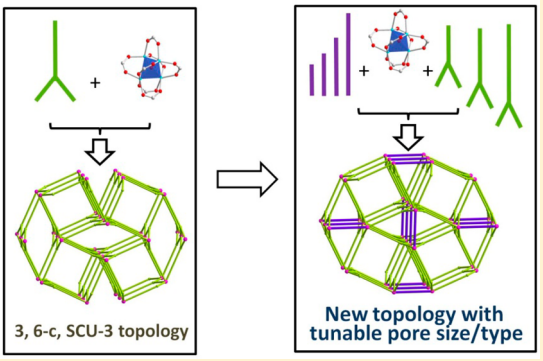

INTRODUCTION

Porous coordination polymers (PCPs), also termed as metal−organic frameworks, are constructed by a variety of ligands and metal ions or clusters. The modular nature of these porous structures and their properties have already shown them to be highly promising materials for a variety of potential applications, especially because of their high surface area and gas-storage capability.[1−8]

In general, to explore the optimal structure for applications in storage or separation, modulation of the pore size/type has been considered as the rational strategy and top choice.[9,10] The systematic modulation in the synthesis of crystalline materials is the alteration of their chemical composition, functionality, and molecular dimensions, that is, without changing the underlying topology.[9] Thus, the selection of the potential framework topology is foremost.

Rht, as the most popular topology, was employed to synthesize highly porous frameworks, because the (3,24)-connected network can be easily achieved by connecting the 24 edges of a cuboctahedron with a C_3 symmetry ligand.[11] A series of isoreticular PCPs has been reported in which the length of the ligands was changed while keeping the cuboctahedron building units. However, they present a difficulty for tuning the pore size and shape simultaneously, because of the preferred coordination geometry between metal center and C_3 symmetry ligand.[7,12−14] *Pcu* topology frameworks, generally associated with the coordination between linear dicarboxylates and $Zn_4O(O_2CR)_6$clusters, show good adjustment for predicted pore metrics by using suitable ligands; however, interpenetration sometimes occurs.[9,15] Therefore, in these related prototypes, their pore sizes can be well-controlled, but they keep the same pore shape. It is very difficult to achieve ideal modulation with traditional structure construction that is based on one ligand. In contrast, introducing a second ligand with a tunable metric into their ternary prototypes would be a feasible method. For example, in pillared-layer structures the length of the channel cross section can be changed, but the modification of their breadth subject to layer structures is generally difficult.[16−18] In addition, a series of PCPs that is formed by coordination between $Zn_4O(O_2CR)_6$ clusters and the mixture of dicarboxylate and tricarboxylate ligands exhibits different topologies, such as *muo, toz, umt*, or *ith-d*, even though their general formulas are same $(Zn_4O(L^2)(L^3)_{4/3}$ (L^3 = tricarboxylate)).[4,19−22] Very recently, a new platform of *ncb* topology has been reported that demonstrates systematic changes in pore parameters and properties of this series of frameworks; however, the connectivity of such kind frameworks was constrained by the similar lengths of the two cooperated ligands.[10] Therefore, in short, understanding the construction principle of molecular building blocks and how to modulate systematically the pore size/shape remains unrealized thus far.

After understanding the 4,8-connected PCP with *scu* topology,[23−26] we found that the 3,6-connected subnet with *scu*-3 topology may be a candidate for precise pore design and control.[27−29] The 3,6-connected framework can be easily prepared from a tricarboxylate ligand and $Zn_4O(O_2CR)_6$ cluster,[30] and also it is possible for the cluster to be coordinated by some terminal molecules.[31] Thus, we believe that if we can insert a linear ligand between adjacent Zn_4O clusters, a 3,7-

Received: November 1, 2014
Published: January 16, 2015

DOI: 10.1021/ic502643m
Inorg. Chem. 2015, 54, 1645−1649

connected framework with unprecedented topology should be generated, and most importantly, we can finely control the porosity and pore size/type by employing the matrix of the cooperated dicarboxylates and tricarboxylates with different length ratios (Scheme 1).

Scheme 1. Strategy for Precise Design of a New Topology Framework with Systematically Tunable Pore Size and Type

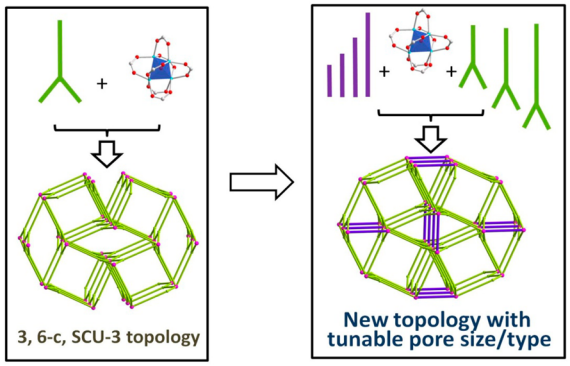

EXPERIMENTAL SECTION

Syntheses of the Ligands and PCPs. General procedures of the experiment for ligands and PCPs syntheses can be found in the Supporting Information.

Single-Crystal X-ray Study. Single-crystal X-ray diffraction data were measured on a Bruker Smart Apex CCD diffractometer at 173 K using graphite monochromated Mo Kα radiation (λ = 0.710 73 Å). Data reduction was made with the Bruker Saint program. The structures were solved by direct methods and refined with full-matrix least-squares technique using the SHELXTL package.[32] Non-hydrogen atoms were refined with anisotropic displacement parameters during the final cycles. Organic hydrogen atoms were placed in calculated positions with isotropic displacement parameters set to 1.2 × U_{eq} of the attached atom. The hydrogen atoms of the ligand water molecules could not be located but are included in the formula. The unit cell includes a large region of disordered solvent molecules, which could not be modeled as discrete atomic sites. We employed PLATON/SQUEEZE[33,34] to calculate the diffraction contribution of the solvent molecules and, thereby, to produce a set of solvent-free diffraction intensities; structures were then refined again using the data generated. Crystal data are summarized in Supporting Information, Table S1.

Gas Sorption Measurements. Before the gas sorption, ~90 mg of sample was activated at 140 °C for 30 h by using the "outgas" function of the surface area analyzer. Ultrahigh-purity grade, N_2, CH_4 (>99.999%), and CO_2 gases (99.995% purity) were used throughout the adsorption experiments. Low-pressure N_2 adsorption measurements (as high as 1 bar) were performed on Micromeritics ASAP 2020 M+C surface area analyzer. A part of N_2 sorption isotherm was fitted to Brunauer–Emmett–Teller (BET) equation to estimate their BET surface area. The pore size distribution was obtained from the density functional theory method in the Micromeritics ASAP2020 software package based on the N_2 sorption at 77 K. High-pressure adsorption of CH_4 and CO_2 were measured using an IGA-003 gravimetric adsorption instrument (Hiden-Isochema, U.K.) over a pressure range of 0–10 bar at 298 and 273 K, respectively.

Selectivity Prediction for Binary Mixture Adsorption. Ideal adsorbed solution theory (IAST) was used to predict binary mixture adsorption from the experimental pure-gas isotherms.[35,36] To perform the integrations required by IAST, the single-component isotherms should be fitted by a proper model. There is no restriction on the choice of the model to fit the adsorption isotherms; however, data over the pressure range under study should be fitted very precisely.[37,38] Several isotherm models were tested to fit the experimental pure isotherms for CH_4 and CO_2 of **IIa** and **IIc**, and the dual-site Langmuir–Freundlich equation was found to have the best fit to the experimental data:

$$q = q_{m1}\cdot\frac{b_1\cdot P^{1/n_1}}{1 + b_1\cdot P^{1/n_1}} + q_{m2}\cdot\frac{b_2\cdot P^{1/n_2}}{1 + b_2\cdot P^{1/n_2}} \quad (1)$$

Here, P is the pressure of the bulk gas at equilibrium with the adsorbed phase (kPa), q is the adsorbed amount per mass of adsorbent (mmol/g), q_{m1} and q_{m2} are the saturation capacities of sites 1 and 2 (mmol/g), b_1 and b_2 are the affinity coefficients of the sites (1/kPa), and n_1 and n_2 are measures of the deviations from an ideal homogeneous surface. Supporting Information, Figures S33 and S34 show that the dual-site Langmuir–Freundlich equation fits the single-component isotherms extremely well. The R_2 values for all of the fitted isotherms were over 0.9997. Hence, the fitted isotherm parameters were applied to perform the necessary integrations in IAST.

RESULTS AND DISCUSSION

Synthesis and Crystal Structure. To confirm our idea, herein, an *scu*-3 topology PCP (named as **I**) with a seven-connected cluster ($Zn4O(O_2CR)_6(CH_3COO)$) was successfully synthesized based on a C_{2v} symmetry tricarboxylate ligand. Encouraged by the result of the first step, three C_{2v} symmetry tricarboxylate ligands with different degrees of vertex desymmetrization and four linear dicarboxylate ligands were selected for the large-scale matrix synthesis (3 × 4) (See Supporting Information). Structure analysis, X-ray diffraction, and ^{1}H NMR show that 10 of the highly porous isostructures (named as **Ia** to **Id**, **IIa** to **IId**, and **IIIc** to **IIId**; detailed definitions are in the Supporting Information) with systematically changed pore size/type were constructed without the limitation of similar lengths of the ligands; also, the layer structures determined the pore widths. Interestingly, **IIa** with a slight change of pore environment shows increased ability for selective capture of CO_2 over CH_4 (11.7–21.3 at 298 K; 17.8–36.3 at 273 K) compared with that of **IIc**. Therefore, our strategy facilitates a promising platform for the development of reticular chemistry and also facilitates the convenient syntheses of materials with suitable pores for expired applications.

To confirm our hypothesis, we tried to prepare a 3,6-connected *scu*-3 topology framework at first. In general, the tricarboxylate ligand combining as a six-connected node would possibly form this type framework. However, the node of this kind of framework must have an extra space for terminally coordinated molecules. This is because the space will allow us to insert a pillar between adjacent nodes for the next design. Six-connected Zn_4O clusters with terminal coordinated solvent molecules would satisfy our requirement (Figure. 1). In addition, the coordination around the Zn_4O cluster by high symmetry ligands, such as H_3BTB, usually leads to an average coordination space for six carboxylate groups, and thus, it is difficult to leave space for terminal molecules, even though the system contains two types of ligands. Thus, a tricarboxylate ligand with lower symmetry, such as C_{2v}, would be the ideal candidate, because the lower symmetry of the ligands usually results in a nonuniformity of the coordination geometry.[39,40]

Solvothermal reaction of $Zn(NO_3)_2\cdot 3H_2O$ and a C_{2v} symmetry H_3L^1 in *N*,*N*-dimethylacetamide (DMA) containing HNO_3 afforded needlelike crystals of $[Zn_4O(L^1)_2\cdot CH_3COO\cdot (NH_2CH_3)]\cdot x$G (**I**) (G = solvent molecule), which crystallizes in the $P_{21/n}$ space group with a = 10.316(2) Å, b = 26.096(5) Å, c = 27.889(6) Å, and β = 3.78(3)°. As expected, the crystal structure of **I** contains the Zn_4O cluster, which was bridged by six carboxylate groups from L^1 ligands and another terminal

DOI: 10.1021/ic502643m
Inorg. Chem. 2015, 54, 1645–1649

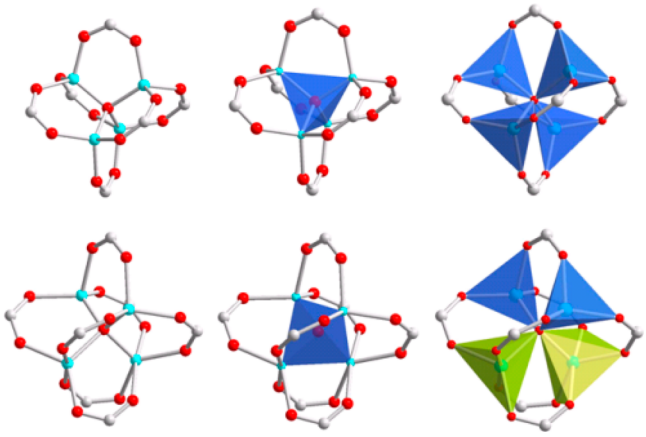

Figure 1. Comparison of coordination geometry of six- (upper) and seven- (bottom) connected Zn_4O clusters. Blue polyhedrons are tetrahedrons, and green polyhedrons are pentahedrons.

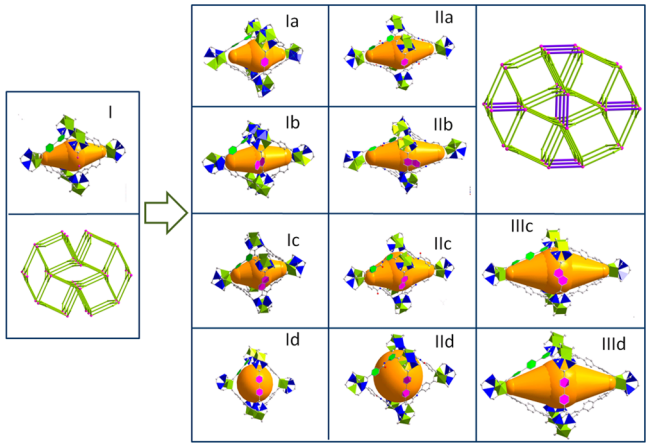

Figure 2. Crystal structures and topology of pore systems. Perspective views of the octahedral building units with systematically adjusted pore size/type (yellow) of series isoreticular PCPs. The tricarboxylate ligands and linear dicarboxylate ligands are highlighted by green and pink colors.

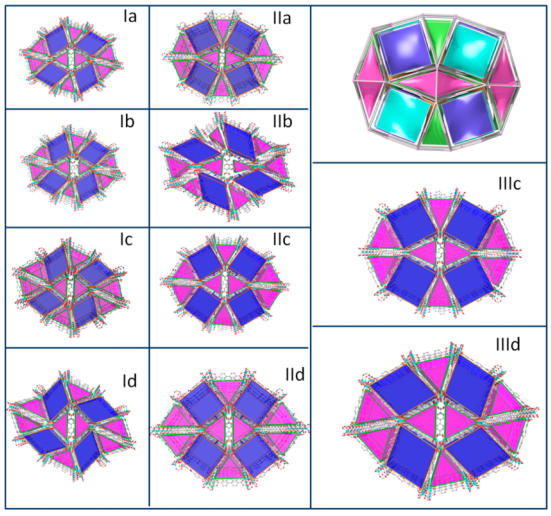

Figure 3. Perspective views of the square (blue) and triangular (pink) channels with systematically adjusted window aperture and type of these series of isoreticular PCPs. Top right shows the tilings of this series of frameworks.

acetic acid. Thus, the coordination numbers for two zinc centers are four, and another two are five. Interestingly, these four zinc atoms still form a tetrahedron. In this structure, each ligand connects three clusters, in turn, generating a three-dimensional 3,6-*c* network with *scu*-3 topology. There are two types of rhombus channels along the *a*-axis, as well as the circular channels along (0 1 1) in **I**. In addition, the pore channels are blocked by the $[Me_2NH_2]^+$ cations for charge balance. $[Me_2NH_2]^+$ cations come from the hydrolysis of DMA solvent during PCP synthesis[41] despite the fact that the total accessible pore volume of **I** was estimated to be 62.2% by PLATON, indicating the highly porous template for the next synthesis. In addition, the phase purity of **I** was confirmed by the powder X-ray diffraction pattern.

On the basis of structure **I**, we attempted to insert a pillar with a different length between the adjacent Zn_4O clusters for systematic tuning of the pore size/type in a series of PCPs having the same underlying topology. Solvothermal reactions of $Zn(NO_3)_2{\cdot}3H_2O$, H_3L^1, and four linear ligands (terephthalic acid: H_2BDC, 1,4-naphtha-lenedicarboxylic acid: 1,4-H_2NDC, 2,6-naphthalenedicarboxylic acid: 2,6-H_2NDC and 4,4′-biphenyldicarboxylic acid: H_2BPDC) in DMA or DMA/DEF (DEF = *N*,*N*-diethylformamide) provided four needlelike crystals (**Ia**, **Ib**, **Ic**, and **Id**). Single-crystal X-ray studies reveal that all of them adopt the Zn_4O cluster as their nodes. Importantly and also as expected, the cluster was coordinated by six carboxylates from tricarboxylate ligands and one carboxylate from the dicarboxylate ligands. Thus, the four generated structures exhibited systematic and simultaneous tuning of pore size/type. To expand the systematic tuning of pore properties, we designed another two tricarboxylate ligands with different lengths at the 4′-position. The generated six structures (**IIa** to **IId**, **IIIc** to **IIId**) also adopt the same coordination mode as the above four PCPs (Figure 2). Therefore, here, not only the pore sizes (6.8−11. 2 Å; 17.0−29.0 Å; 12.5−22.8 Å; 11.9−24.5 Å), and anisotropy of pore types but also the potentially accessible pore volumes (57−71%) were finely controlled and predesigned (Figures 3 and 4). For simplification, L^{3-} ligands and L^{2-} ligands were simplified as 3- and 2-connected linkers, whereas the $Zn_4O(COO)_7$ cluster is a seven-connected node. As a result, these 10 PCPs show a three-dimensional 3,7-*c* net with the Schläfli symbol of $\{4.5^2\}2\{4^2{\cdot}5^5{\cdot}6^{10}{\cdot}8^4\}$, which has not been encountered in PCP chemistry nor experimentally/theoretically predicted. Powder X-ray diffraction patterns reflect well the phase purity of the as-synthesized frameworks. The ratio of the mixed ligands in each crystal was further confirmed by the ^1H NMR spectra. Thermal gravimetric analyses (TGA) indicate that all PCPs are stable up to 400 °C under N_2 (see Supporting Information).

To compare the function of well-controlled pore size/type, **IIa** and **IIc** were selected as representatives, because their pore sizes/type are almost identical. CO_2 and CH_4 adsorption isotherms were collected at 273 and 298 K, respectively (Figures 5 and 6). Ideal adsorbed solution theory (IAST) was employed to predict multicomponent adsorption behaviors from the experimental pure-gas isotherms. The predicted adsorption selectivities for equimolar CO_2/CH_4 mixtures in **IIa** and **IIc** as a function of bulk pressure are presented in Figure. 7. Interestingly, the simulated selectivity of **IIa** is almost two times higher than that of **IIc** under the same conditions (from 11.7 to 21.3 at 298 K and 17.8 to 36.3 at 273 K), reflecting the function of changed pore sizes.

DOI: 10.1021/ic502643m
Inorg. Chem. 2015, 54, 1645−1649

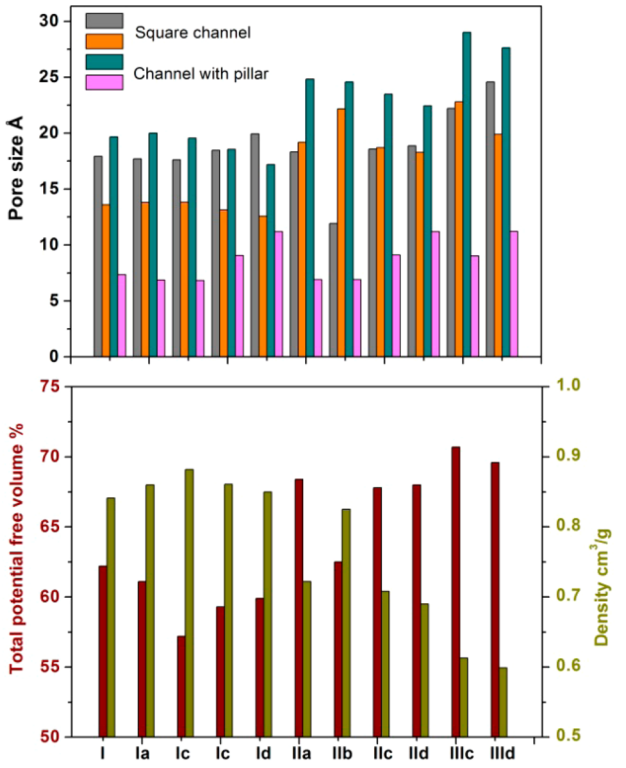

Figure 4. Systematic modulation of pore parameters in this series of PCPs: (a) potential accessible pore volumes and framework densities; (b) pore sizes of two types of channels.

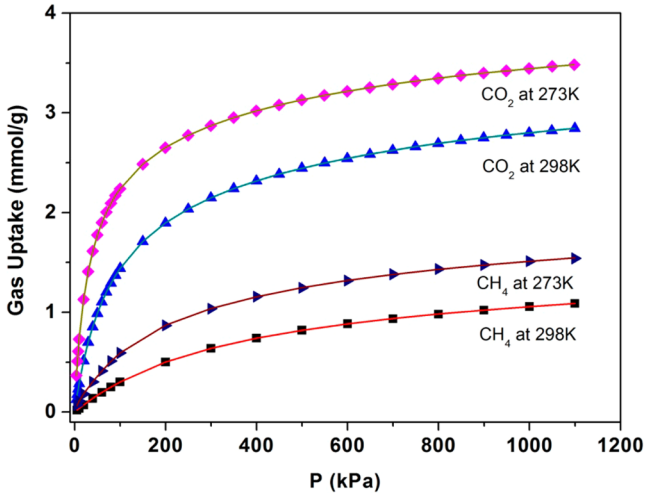

Figure 5. High-pressure gas adsorption isotherms (dot) and the dual-site Langmuir–Freundlich fit lines (line) of CO_2 and CH_4 in **IIa**.

In summary, we present a rational and promising platform for predesign and systematic synthesis of highly porous PCPs. This series of isoreticular frameworks shows the unprecedented topology underlying the 3 × 4 ligand matrix. Importantly, their potential accessible pore volumes, sizes, and also pore shapes were simultaneously and systematically controlled. The increased selectivity of **IIa** shows the functional ability of tuned pore properties. Therefore, our work will further facilitate research on PCPs, in particular, the fine control of PCPs structures for the expired application.

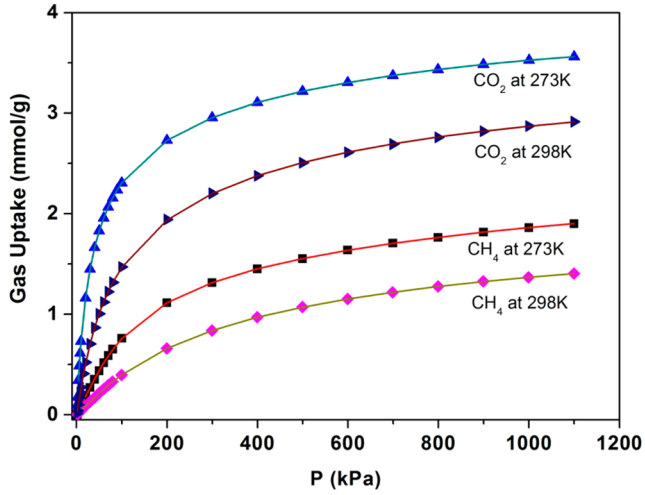

Figure 6. High-pressure gas adsorption isotherms (dot) and the dual-site Langmuir–Freundlich fit lines (line) of CO_2 and CH_4 in **IIc**.

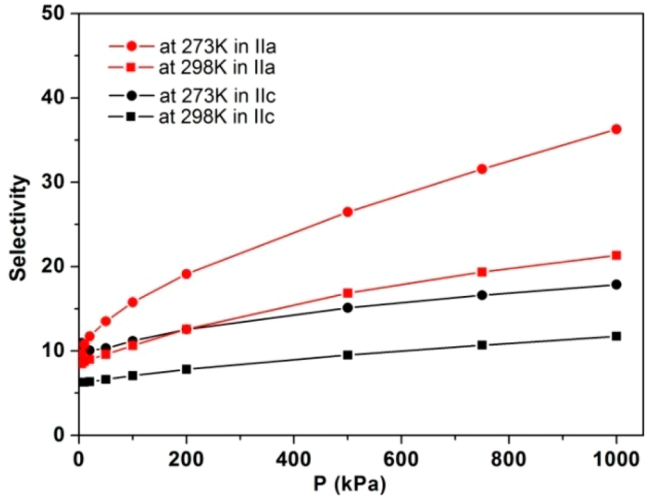

Figure 7. IAST predicted selectivity of CO_2 over CH_4 of **IIa** and **IIc** at 273 and 298 K, respectively.

■ ASSOCIATED CONTENT

Ⓢ Supporting Information

Materials and equipment used, details of syntheses, characterization of polymers, tabulated crystal data and structure refinement for complexes, illustrations of framework of I, topology of I, tiling of I, open channel in IIa structure, topology of Ia-IIId, tiling transformation from I to Ia, TG curves of PCP series, X-ray diffraction patterns, 1H NMR spectra, illustrated BET data, calculated pore size distributions. This material is available free of charge via the Internet at http://pubs.acs.org. CCDC Nos. of these 11 PCPs: 1016123–1016133.

■ AUTHOR INFORMATION

Corresponding Authors

*E-mail: kitagawa@icems.kyoto-u.ac.jp. (S.K.)
*E-mail: duanjingui@njtech.edu.cn. (J.D.)

Notes

The authors declare no competing financial interest.

DOI: 10.1021/ic502643m
Inorg. Chem. 2015, 54, 1645–1649

■ ACKNOWLEDGMENTS

The authors gratefully acknowledge support from the Natural Science Foundation of China (No. 21301148), the Advanced Catalytic Transformation Program for Carbon Utilization (ACT-C), the PRESTO Program of the Japan Science and Technology Agency (JST), and MEXT Project for Developing Innovation Systems Regional Innovation Strategy Support Program Kyoto Next-Generation Energy System Creation Strategy (MEXT: the Ministry of Education, Culture, Sports, Science and Technology of Japan. The Institute for Integrated Cell-Material Sciences (iCeMS) is supported by the World Premier International Research Initiative (WPI).

■ REFERENCES

(1) Matsuda, R.; Kitaura, R.; Kitagawa, S.; Kubota, Y.; Belosludov, R. V.; Kobayashi, T. C.; Sakamoto, H.; Chiba, T.; Takata, M.; Kawazoe, Y.; Mita, Y. *Nature* **2005**, *436*, 238−241.
(2) Kondo, M.; Yoshitomi, T.; Seki, K.; Matsuzaka, H.; Kitagawa, S. *Angew.Chem., Int. Ed.* **1997**, *36*, 1725−1727.
(3) Li, H.; Eddaoudi, M.; O'Keeffe, M.; Yaghi, O. M. *Nature* **1999**, *402*, 276−279.
(4) Furukawa, H.; Ko, N.; Go, Y. B.; Aratani, N.; Choi, S. B.; Choi, E.; Yazaydin, A. O.; Snurr, R. Q.; O'Keeffe, M.; Kim, J.; Yaghi, O. M. *Science* **2010**, *329*, 424−428.
(5) Farha, O. K.; Yazaydin, A. O.; Eryazici, I.; Malliakas, C. D.; Hauser, B. G.; Kanatzidis, M. G.; Nguyen, S. T.; Snurr, R. Q.; Hupp, J. T. *Nat. Chem.* **2010**, *2*, 944−948.
(6) Vaidhyanathan, R.; Iremonger, S. S.; Shimizu, G. K. H.; Boyd, P. G.; Alavi, S.; Woo, T. K. *Science* **2010**, *330*, 650−653.
(7) Yan, Y.; Yang, S. H.; Blake, A. J.; Schroder, M. *Acc. Chem. Res.* **2014**, *47*, 296−307.
(8) Jiang, H. L.; Xu, Q. *Chem. Commun.* **2011**, *47*, 3351−3370.
(9) Eddaoudi, M.; Kim, J.; Rosi, N.; Vodak, D.; Wachter, J.; O'Keeffe, M.; Yaghi, O. M. *Science* **2002**, *295*, 46−472.
(10) Zhang, Y. B.; Zhou, H. L.; Lin, R. B.; Zhang, C.; Lin, J. B.; Zhang, J. P.; Chen, X. M. *Nat. Commun.* **2012**, *3*, 642−651.
(11) Nouar, F.; Eubank, J. F.; Bousquet, T.; Wojtas, L.; Zaworotko, M. J.; Eddaoudi, M. *J. Am. Chem. Soc.* **2008**, *130*, 1833−1834.
(12) Yan, Y.; Lin, X.; Yang, S. H.; Blake, A. J.; Dailly, A.; Champness, N. R.; Hubberstey, P.; Schroder, M. *Chem. Commun.* **2009**, 1025−1027.
(13) Zhao, D.; Yuan, D. Q.; Sun, D. F.; Zhou, H. C. *J. Am. Chem. Soc.* **2009**, *131*, 9186−9187.
(14) Zheng, B.; Bai, J.; Duan, J.; Wojtas, L.; Zaworotko, M. *J. Am. Chem. Soc.* **2011**, *133*, 748−751.
(15) Wee, L. H.; Lohe, M. R.; Janssens, N.; Kaskel, S.; Martens, J. A. *J. Mater. Chem.* **2012**, *22*, 13742−13746.
(16) Kondo, M.; Okubo, T.; Asami, A.; Noro, S.; Yoshitomi, T.; Kitagawa, S.; Ishii, T.; Matsuzaka, H.; Seki, K. *Angew. Chem., Int. Ed.* **1999**, *38*, 140−143.
(17) Kitaura, R.; Fujimoto, K.; Noro, S.; Kondo, M.; Kitagawa, S. *Angew. Chem., Int. Ed.* **2002**, *41*, 133−135.
(18) Maji, T. K.; Uemura, K.; Chang, H. C.; Matsuda, R.; Kitagawa, S. *Angew. Chem., Int. Ed.* **2004**, *43*, 3269−3272.
(19) Koh, K.; Wong-Foy, A. G.; Matzger, A. J. *Angew. Chem., Int. Ed.* **2008**, *47*, 677−680.
(20) Klein, N.; Senkovska, I.; Gedrich, K.; Stoeck, U.; Henschel, A.; Mueller, U.; Kaskel, S. *Angew. Chem., Int. Ed.* **2009**, *48*, 9954−9957.
(21) Koh, K.; Wong-Foy, A. G.; Matzger, A. J. *J. Am. Chem. Soc.* **2009**, *131*, 4184−4185.
(22) Koh, K.; Wong-Foy, A. G.; Matzger, A. J. *J. J. Am. Chem. Soc.* **2010**, *132*, 15005−15010.
(23) Zhu, Y. F.; Fang, Y.; Kaskel, S. *J. Phys. Chem. C* **2010**, *114*, 16382−16388.
(24) Du, H. C.; Tang, L. J.; Kaskel, S. *J. Phys. Chem. C* **2009**, *113*, 1329−1339.
(25) Ma, L. Q.; Mihalcik, D. J.; Lin, W. B. *J. Am. Chem. Soc.* **2009**, *131*, 4610−4611.
(26) Hirscher, M. *Angew. Chem., Int. Ed.* **2011**, *50*, 581−582.
(27) Feng, D. W.; Gu, Z. Y.; Li, J. R.; Jiang, H. L.; Wei, Z. W.; Zhou, H. C. *Angew. Chem., Int. Ed.* **2012**, *51*, 10307−10310.
(28) Rao, X. T.; Cai, J. F.; Yu, J. C.; He, Y. B.; Wu, C. D.; Zhou, W.; Yildirim, T.; Chen, B. L.; Qian, G. D. *Chem. Commun.* **2013**, *49*, 6719−6721.
(29) Makal, T. A.; Wang, X.; Zhou, H. C. *Cryst. Growth Des.* **2013**, *13*, 4760−4768.
(30) Chae, H. K.; Siberio-Perez, D. Y.; Kim, J.; Go, Y.; Eddaoudi, M.; Matzger, A. J.; O'Keeffe, M.; Yaghi, O. M. *Nature* **2004**, *427*, 523−527.
(31) Duan, J.; Bai, J.; Zheng, B.; Li, Y.; Ren, W. *Chem. Commun.* **2011**, *47*, 2556−2558.
(32) Sheldrick, G. M. *Acta Crystallogr., Sect. A* **2008**, *64*, 112−122.
(33) Vandersluis, P.; Spek, A. L. *Acta Crystallogr., Sect A* **1990**, *46*, 194−201.
(34) Spek, A. L. *J. Appl. Crystallogr.* **2003**, *36*, 7−13.
(35) Bae, Y. S.; Mulfort, K. L.; Frost, H.; Ryan, P.; Punnathanam, S.; Broadbelt, L. J.; Hupp, J. T.; Snurr, R. Q. *Langmuir* **2008**, *24*, 8592−8598.
(36) Duan, J.; Higuchi, M.; Horike, S.; Foo, M.; Rao, K.; Inubushi, Y.; Fukushima, T.; Kitagawa, S. *Adv. Funct. Mater.* **2013**, *23*, 3525−3530.
(37) Babarao, R.; Hu, Z. Q.; Jiang, J. W.; Chempath, S.; Sandler, S. I. *Langmuir* **2007**, *23*, 659−666.
(38) Goetz, V.; Pupier, O.; Guillot, A. *Adsorption* **2006**, *12*, 55−63.
(39) Duan, J.; Yang, Z.; Bai, J.; Zheng, B.; Li, Y.; Li, S. *Chem. Commun.* **2012**, *48*, 3058−3060.
(40) Schnobrich, J. K.; Lebel, O.; Cychosz, K. A.; Dailly, A.; Wong-Foy, A. G.; Matzger, A. J. *J. Am. Chem. Soc.* **2010**, *132*, 13941−13948.
(41) Yu, L. C.; Liu, S. L.; Liang, E. X.; Wen, C. L. *J. Coord. Chem.* **2007**, *60*, 2097−2105.

DOI: 10.1021/ic502643m
Inorg. Chem. 2015, 54, 1645−1649